2-16-2007

In Vivo Membrane Topology of Escherichia Coli SecA ATPase Reveals Extensive Periplasmic Exposure of Multiple Functionally Important Domains Clustering on One Face of SecA

Don Oliver
Wesleyan University, doliver@wesleyan.edu

THE JOURNAL OF BIOLOGICAL CHEMISTRY VOL. 282, NO. 7, pp. 4661–4668, February 16, 2007

In Vivo Membrane Topology of *Escherichia coli* SecA ATPase Reveals Extensive Periplasmic Exposure of Multiple Functionally Important Domains Clustering on One Face of SecA*[S]

Received for publication, November 22, 2006 Published, JBC Papers in Press, December 13, 2006, DOI 10.1074/jbc.M610828200

Lucia B. Jilaveanu and Donald B. Oliver[1]

From the Department of Molecular Biology and Biochemistry, Wesleyan University, Middletown, Connecticut 06459

The Sec-dependent protein translocation pathway promotes the transport of proteins into or across the bacterial plasma membrane. SecA ATPase has been shown to be a nanomotor that associates with its protein cargo as well as the SecYEG channel complex and to undergo ATP-driven cycles of membrane insertion and retraction that promote stepwise protein translocation. Previous studies have shown that both the 65-kDa N-domain and 30-kDa C-domain of SecA appear to undergo such membrane cycling. In the present study we performed *in vivo* sulfhydryl labeling of an extensive collection of monocysteine *secA* mutants under topologically specific conditions to identify regions of SecA that are accessible to the *trans* side of the membrane in its membrane-integrated state. Our results show that distinct regions of five of six SecA domains were labeled under these conditions, and such labeling clusters to a single face of the SecA structure. Our results demarcate an extensive face of SecA that interacts with SecYEG and is in fluid contact with the protein-conducting channel. The observed domain-specific labeling patterns should also provide important constraints on model building efforts in this dynamic system.

The major Sec-dependent protein translocation pathway of Eubacteria, which is essential for both protein secretion and integral membrane protein insertion, has been subjected to intensive investigation for over two decades. Its core components consist of the SecA ATPase nanomotor along with SecYEG, the presumed protein-conducting channel (reviewed in Refs. 1 and 2). Peripheral components such as the export-specific SecB chaperone, which maintains preproteins in a loosely folded export-competent state and transfers them to SecA, along with the integral membrane SecDF complex, which plays an as yet unknown role in the process, are important for rapid and efficient protein translocation (3–5).

The protein translocation reactions are organized by the SecA ATPase nanomotor, a complex protein that consists of a 65-kDa N-domain and a 30-kDa C-domain (6, 7). The N-domain consists of two nucleotide-binding domains, NBF-I and NBF-II,[2] which together form a high affinity nucleotide-binding cleft, whereas a protein substrate-binding domain (PPXD) is attached to NBF-I and is subject to its modulation (8–10). The C-domain consists of a central helical scaffold domain (HSD), an organizing center upon which the various other domains of SecA reside, a helical wing domain (HWD), and a carboxyl-terminal region (CTR) that contains both acidic phospholipid and SecB binding sites (11, 12).

Soluble, peripheral membrane and integral membrane pools of SecA have been described previously (13). Membrane-bound SecA consists of a pool bound via acidic phospholipids as well as one bound with nanomolar affinity to SecYEG, the SecA receptor (14, 15). Both free and membrane-bound SecA have the capacity to interact directly with preproteins or to receive them via transfer from the SecB-preprotein complex (14, 16, 17). By simultaneously binding both protein substrates as well as SecYEG, SecA is able to initiate protein translocation.

The dominant model for Sec-dependent protein translocation posits that a mobile region of SecA undergoes ATP-driven cycles of membrane insertion and retraction at SecYEG to promote the stepwise translocation of proteins (referred to as SecA membrane cycling) (18). This model was originally based on the observation that both the N- and C-domains of SecA appeared to undergo membrane insertion in an ATP-, preprotein-, and SecYEG-dependent fashion based on their protease-resistant state as well as their accessibility to labeling reagents that specifically label only the exterior side of the membrane (6, 18–21). SecA has also been shown to undergo a default membrane insertion reaction in the presence of nonhydrolyzable ATP analogs (22). However, the additional observation that the protease-resistant state of the C-domain could also be induced in the presence of micellar SecYEG and a nonhydrolyzable ATP analog, under conditions in which SecYEG is degraded to small peptides, has led to the alternative suggestion that these translocation ligands simply induce a stable SecA conformational state (23).

* This work was supported by Grant GM42033 from NIGMS, National Institutes of Health. The costs of publication of this article were defrayed in part by the payment of page charges. This article must therefore be hereby marked "*advertisement*" in accordance with 18 U.S.C. Section 1734 solely to indicate this fact.

[S] The on-line version of this article (available at http://www.jbc.org) contains supplemental Figs. S1–S3.

[1] To whom correspondence should be addressed: Molecular Biology and Biochemistry Dept., Wesleyan University, Middletown, CT 06457. Tel.: 860-685-3556; Fax: 860-685-2141; E-mail: doliver@wesleyan.edu.

[2] The abbreviations used are: NBF, nucleotide-binding domain; PPXD, preprotein-binding domain; HSD, helical scaffold domain; HWD, helical wing domain; CTR, carboxyl-terminal region; AMS, 4-acetamido-4′-maleimidyl-stilbene-2,2′-disulfonic acid; MPB, 3-(*N*-maleimido-propinyl)biocytin; P300, membrane fraction; RSO, right-side-out membrane vesicles; S300, soluble fraction; M/S, moderate to strong.

The structure of SecYEG protein, its conformational flexibility, and the dimensions and topology of the protein-conducting channel should provide important clues into the molecular basis of SecA membrane cycling. However, these topics have been the source of considerable controversy. Monomeric, dimeric, and tetrameric states for SecYEG have been detected in various biochemical and structural studies in which the presence of SecA, preprotein, and ATP stimulated the formation of dimeric and tetrameric forms of SecYEG (see Refs. 1 and 24 and references contained therein). A small 5–8-Å protein-conducting channel has been proposed to lie within the SecYEG protomer, whereas a much larger channel of ~20 Å would be formed at the interface of SecYEG oligomers in the ring-like structures that have been observed previously (25–28). Recent studies favor the former model. In one study utilizing cryoelectron microscopy reconstruction, a ribosome-nascent chain complex was captured associated with a SecYEG dimer, where one protomer formed the active protein-conducting channel, while the second protomer was in an inactive state (29). In a second study utilizing cysteine-scanning mutagenesis and disulfide bond formation, the translocating polypeptide chain was located exclusively within the central region of SecY (30). Such a narrow channel, which begins with a 20–25-Å opening but narrows to 5–8 Å at the pore ring at the middle of the membrane, would significantly limit both the depth and extent of SecA membrane insertion at SecYEG.

Clearly a high-resolution structure of SecA in its membrane-inserted state at SecYEG with or without a translocation intermediate is required to elucidate the structural dynamics of the translocon. However, given the difficulty in obtaining crystals of dynamic membrane proteins that diffract to atomic dimensions, this approach is likely to be difficult to achieve. The structure of the SecY complex from *Methanocaldococcus jannaschii*, obtained recently, is of limited use, because Archaea do not possess a SecA homolog but instead utilize a signal recognition particle-mediated pathway for protein secretion (25, 31). Therefore, other approaches to obtain such structural information need to be sought.

Cysteine-scanning mutagenesis, combined with either topologically specific sulfhydryl labeling or disulfide bond formation, has been shown to be a powerful method of assessing membrane protein structure and topology. For example, considerable information on the proximity of the different transmembrane helices and cytosolic or periplasmic domains of SecYEG protein has been obtained utilizing this approach (reviewed in Ref. 1). In addition, *in vivo* assessment of the periplasmic accessibility of engineered cysteine residues within an integral membrane protein to membrane-impermeable sulfhydryl reagents has been utilized to derive the topology of membrane transporters in a less invasive manner than through the utilization of more conventional *in vitro* approaches (reviewed in Ref. 32).

Previously we utilized cysteine-scanning mutagenesis along with MPB labeling in RSO to demonstrate that at least three distinct regions within PPXD, NBF-II, and CTR of integral membrane SecA were periplasmically accessible (20). This approach is limited however by the laboriousness of the methodology as well as potential artifacts induced during spheroplating and osmotic rupture, which is a particular concern given the highly dynamic nature of the Sec system. In the present study we have utilized *in vivo* rather than *in vitro* topology labeling to minimize system perturbation and have greatly expanded the number of cysteine mutants that have been examined. Our results provide the first detailed look at the membrane topology of integral membrane SecA protein in a more physiological manner than used previously.

EXPERIMENTAL PROCEDURES

Strains, Plasmids, and Chemicals—*Escherichia coli* BL21.19 (*secA13(Am) supF(Ts) trp(Am) zch::Tn10 recA::CAT clpA::KAN*) is derived from BL21(λDE3) (33) and was used as the host for all *secA*-containing plasmids. Plasmid pT7secA-Cys-0, a derivative of pT7secA2 that has all four cysteine codons within *secA* changed to serine, has been described previously (20); it was used to create the collection of monocysteine *secA* mutants described here utilizing a QuikChange site-directed mutagenesis kit (Stratagene) and appropriate oligonucleotides (Integrated DNA Technologies) as described by the manufacturer. All *secA* mutants were verified by DNA sequence analysis utilizing the DNA sequence facility at the University of Pennsylvania. The efficiency of plating of a given *secA* mutant, obtained by plating an appropriate dilution of an overnight culture of the strain on LB ampicillin (100 μg/ml) plates and incubating them overnight at either 42 or 30 °C, is defined as the ratio of the titer of colonies obtained at 42 °C divided by that obtained at 30 °C × 100%. MPB and AMS were purchased from Molecular Probes. Unless otherwise noted, most other chemicals were reagent grade or better and were obtained from Sigma or a comparable supplier.

In Vivo MPB Labeling of Cells—Each monocysteine *secA* mutant was grown in LB medium supplemented with ampicillin (100 μg/ml) at 42 °C to an A_{600} of 0.65–0.7, after which the culture was chilled rapidly on ice for 10–20 min and then harvested by sedimentation at 7,000 × *g* for 10 min at 4 °C. The cell pellet was resuspended in 0.075 volume of buffer 1 (50 mM Hepes, pH 7.6, 250 mM sucrose, 5 mM EDTA). Where specified, the resuspended culture was incubated with 5 mM AMS at 4 °C for 90 min followed by sedimentation at 20,000 × *g* for 10 min at 4 °C, when the cell pellet was washed and resuspended in an equivalent volume of buffer 1 prior to MPB labeling. In other experiments the resuspended culture was incubated with 0.1% Triton X-100 at 0 °C for 15 min prior to MPB labeling. Biotinylation was performed by incubation with 75 μM MPB for 3 min at 0 °C. Labeling was quenched by the addition of 2-mercaptoethanol to 500 mM and incubation at 0 °C for 5 min followed by sedimentation of cells at 20,000 × *g* for 10 min at 4 °C. The cell pellet was resuspended in an equivalent volume of buffer 2 (50 mM Hepes, pH 7.6, 150 mM NaCl, 5 mM EDTA) supplemented with 200 mM 2-mercaptoethanol. In certain instances the MPB labeling pattern was analyzed directly on total cell protein by the addition of sample buffer (2% SDS, 125 mM Tris-HCl, pH 6.8, 5% 2-mercaptoethanol, 15% glycerol, 0.005% bromphenol blue) followed by SDS-PAGE and immunoblotting as described previously (34). In other cases the MPB labeling pattern was analyzed on subcellular fractions. For this purpose cells were broken by two passages at 8,000 lb/in^2 in a French pressure cell, and unbroken cells were removed by sedimentation at 13,000 ×

g for 10 min at 4 °C, giving rise to the total cleared lysate. Soluble (S300) and membrane (P300) fractions were prepared by sedimentation of the total cleared lysate at 320,000 × *g* for 30 min at 4 °C in a Sorvall RC M100 Micro-Ultracentrifuge. S300 was removed, and P300 was resuspended in one-sixth of the original volume of buffer 2. Following the addition of sample buffer and SDS-PAGE and immunoblotting, visualization of biotinylated proteins utilized streptavidin-conjugated horseradish peroxidase (Molecular Probes) and ECL (Pierce), whereas visualization of SecA content employed primary rabbit anti-SecA antisera and secondary goat anti-rabbit IgG-conjugated horseradish peroxidase (Pierce) and ECL.

RESULTS AND DISCUSSION

Construction of Monocysteine secA Mutants and In Vivo Labeling with MPB—Previous studies have demonstrated the feasibility of performing a topological analysis of membrane proteins utilizing a cysteine-scanning approach combined with *in vivo* labeling with sulfhydryl-reactive reagents (reviewed in Ref. 32). To undertake a similar approach with SecA ATPase, we created an extensive collection of monocysteine *secA* mutants. The mutations were targeted according to four principles. (i) We sought a mutation density that would provide us with detailed topological information on the different SecA domains, resulting in a collection of 63 monocysteine mutants for the 901-amino acid-residue SecA protein. (ii) By inspection of the homologous *Bacillus subtilis* SecA structure (8) (the two proteins have 50% identity at the amino acid sequence level (35, 36)), we attempted to confine our selection of monocysteine substitutions to either surface-accessible residues or residues that are located at domain-domain interfaces; the latter residues could readily become surface-accessible by a change in SecA conformation during its membrane insertion. (iii) To avoid nonfunctional *secA* mutants that would be difficult to grow in a haploid state and that could give rise to spurious results, we utilized an alignment of existing eubacterial SecA protein sequences to avoid highly conserved amino acid residues, and where feasible, we placed the substitution at a site where a naturally occurring cysteine residue was located in one of the SecA homologs. (iv) Finally, we tried to choose amino acid residues that were structurally/chemically similar to cysteine for substitution.

The monocysteine substitutions were made on a plasmid-borne functional copy of the *secA* gene in which its four naturally occurring cysteine codons were substituted with serine (see "Experimental Procedures"). *secA* function was assessed in BL21.19, where chromosomal *secA* expression can be shut off by growth at 42 °C because of the presence of a *secA* amber mutation and a temperature-sensitive amber suppressor (37). Nearly all of our monocysteine *secA* mutants were functional *in vivo* as assessed by the ability of the appropriate plasmid-borne *secA* allele to complement the *secA* amber defect at 42 °C, and they gave rise to plating efficiencies of 25% or greater in general (defined under "Experimental Procedures"). The few monocysteine *secA* mutants that were nonfunctional were not subjected to further analysis in this study.

To label regions of SecA in a topologically specific manner, we grew our strains under conditions in which only the monocysteine-containing *secA* gene copy was expressed at a moderate level (at 42 °C and without isopropyl-1-thio-β-D-galactopyranoside induction), and we employed the readily detectable sulfhydryl-labeling reagent, MPB. Previous studies have shown that when MPB is utilized at low concentrations, it is impermeable to the plasma membrane and can be used to map periplasmically accessible portions of membrane proteins (Refs. 38 and 39; also shown below). The topological specificity of MPB labeling of SecA in RSO has also been demonstrated previously (20). In piloting our experiments we found that analysis of membrane fractions of *in vivo* labeled strains gave better clarity and sensitivity in our Western blots, although it was possible to analyze unfractionated cells directly as well. These procedures allowed us to directly compare the SecA labeling intensities of our different mutants without the use of immunoprecipitation or affinity purification, which complicate comparisons because of the high degree of variability in sample recovery. In addition, we found that by running the SDS-polyacrylamide gels for a longer time, better separation of high molecular weight membrane proteins in the range of SecA was achieved.

By utilizing an MPB concentration and labeling time similar to those used in our previous study, we were able to achieve topologically specific labeling of SecA *in vivo* based on four criteria. (i) Cys-530, which has been shown previously to label strongly with MPB in RSO (20), was strongly labeled under our new regimen when the relevant P300 fraction was examined. By contrast, Cys-0, which lacked any cysteine residues, was not labeled even though both proteins were present at comparable levels (Fig. 1, compare *panels A* and *B*). (ii) Cys-530 labeling was prevented by pretreatment of cells with AMS (Fig. 1*A*), which has been utilized extensively to demonstrate topologically specific labeling by sulfhydryl-reactive reagents because of its membrane impermeability (39). (iii) Cys-530, Cys-350, and Cys-470, which have been shown previously to label strongly, moderately, and weakly, respectively, in RSO (20), gave a similar *in vivo* labeling pattern; furthermore, strong labeling was observed in these latter two cases if the integrity of the plasma membrane was breached by Triton X-100 treatment prior to labeling (Fig. 1*A*). (iv) Finally, only membrane-associated SecA and not soluble SecA was labeled *in vivo* unless the plasma membrane was permeabilized by Triton X-100 treatment prior to labeling (Fig. 1, compare *panels A* and *C*, which contain the P300 and S300 fractions, respectively). The single, prominent, MPB-labeled, soluble protein of unknown identity in S300 fractions was presumably periplasmic in origin and was unrelated to SecA. We noted, as previous authors have done, that there was a relatively small number of MPB-labeled membrane proteins in our P300 (Fig. 1*A*) due to the fact that most naturally occurring cysteine residues that are accessible to the *trans* side of the membrane often participate in disulfide bond formation (40). This circumstance makes *in vivo* labeling with sulfhydryl-reactive reagents ideal when combined with a cysteine-scanning mutagenesis approach, provided that expression levels of the test membrane protein are sufficient for ready detection.

To demonstrate that our procedure labeled SecYEG-bound SecA protein, we investigated the SecYEG dependence of MBP labeling. For this purpose we compared the MPB labeling efficiency of BL21.19 (pBBsecA-his), which contains *secA* on a low

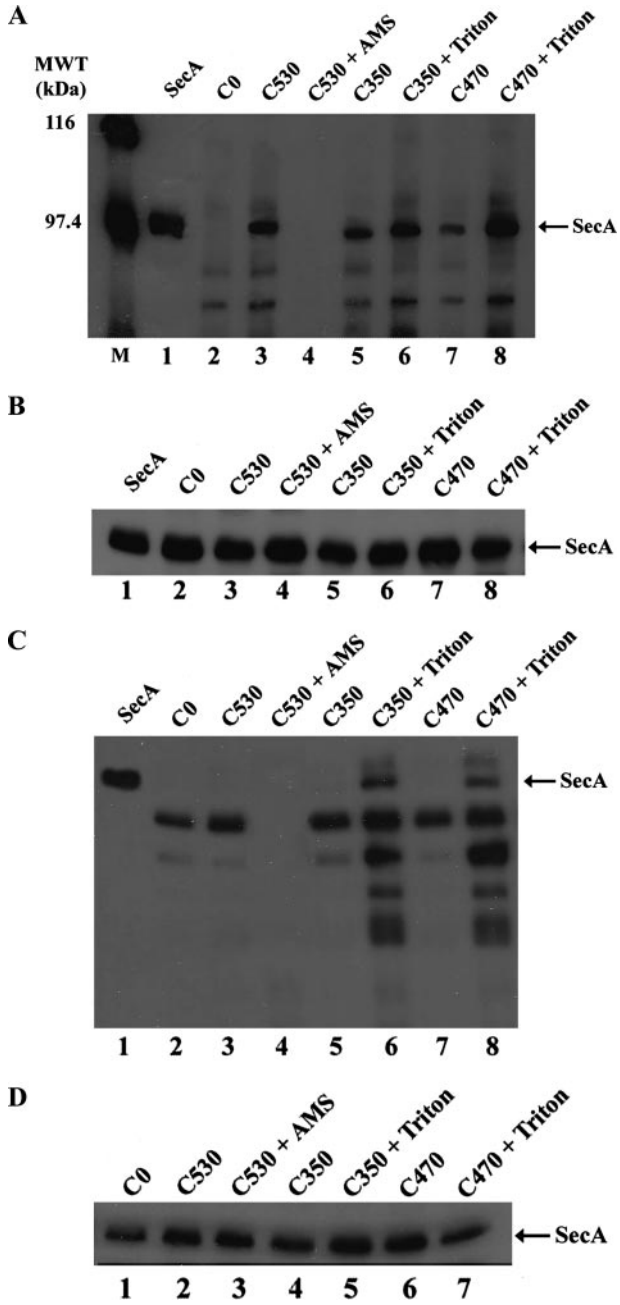

FIGURE 1. **Specificity of *in vivo* MPB labeling methodology.** *In vivo* MPB labeling was performed as described under "Experimental Procedures." *A*, Western blot probed with streptavidin-conjugated horseradish peroxidase. *Lane M*, contains molecular mass markers of 116 and 97.4 kDa. *Lane 1*, 1 μg of purified wild-type SecA labeled with 75 μM MPB in buffer 2 at 0 °C for 3 min. *Lanes 2–8*, 10 μl of P300 of the indicated MPB-labeled strain. Each monocysteine *secA* mutant is indicated by the *letter C* followed by the *residue number* that contains the cysteine substitution. *Lane 2*, BL21.19 (pT7secA-Cys-0). *Lanes 3 and 4*, BL21.19 (pT7secA-Cys-530) labeled without and with AMS pretreatment, respectively. *Lanes 5 and 6*, BL21.19 (pT7secA-Cys-350) labeled in the absence and presence of 0.1% Triton X-100, respectively. *Lanes 7 and 8*, BL21.19 (pT7secA-Cys-470) labeled in the absence and presence of 0.1% Triton X-100, respectively. *B*, similar to *A* except that the Western blot was probed with SecA antisera. *C*, similar to *A* except that 10 μl of S300 of each strain was analyzed in the Western blot that was probed with streptavidin-conjugated horseradish peroxidase. *D*, similar to *C* except that the Western blot was probed with SecA antisera.

copy number plasmid (34), with that of BL21.19 (pBBsecA-his, pET610). Plasmid pET610 overproduces SecYEG protein, utilizing the powerful Trc promoter (41). The results of this analysis showed that the specific activity of MPB labeling of SecA was increased 2.6-fold by SecYEG overproduction after accounting for a 34% lower SecA level in BL21.19 (pBBsecA-his, pET610) compared with BL21.19 (pBBsecA-his) (supplemental Fig. S1). Although the observed increase in specific activity of SecA labeling appears to be lower than the increase in SecYEG overproduction, we have shown previously that only a fraction of overproduced SecYEG protein properly assembles in the membrane where it gives rise to an increase in SecA high affinity binding sites and SecA-dependent translocation ATPase activity (42). However, we cannot rule out the possibility that some of the MPB-labeled residues of SecA arose from periplasmic exposure of a phospholipid-bound pool of SecA, although such speculation is inconsistent with the extractability of this pool of SecA by reagents that classically remove only peripherally bound membrane proteins (15). In addition, this latter concern is inconsistent with our data given below.

Data Analysis—Analysis of the MPB labeling pattern of 63 monocysteine *secA* mutants is given in Table 1. To ensure that our data were consistent, we performed two or more independent experiments (with separate Western blots) for each mutant, and positive and negative controls (Cys-530 and Cys-0, respectively) were included with each experiment. Given a modest degree of variability in labeling intensity and a continuum in labeling strength between strongly and moderately labeled mutants, we divided the labeling patterns into three groups: moderately to strongly labeled, weakly labeled, and unlabeled (M/S, W, and U, respectively, in Table 1). This scoring system provided a fairer representation of our data and eliminated a potentially more subjective bias. A large proportion (43%) of the SecA monocysteine residues are contained within the M/S group, a similar proportion (46%) are contained within the unlabeled (U) group, and the remainder (11%) resides within the weakly labeled (W) group.

Two different types of controls were used to ensure the quality of the entire data set. First, to confirm the topological specificity of labeling of the M/S group of mutants, we compared their labeling pattern in the absence and presence of AMS. Inclusion of AMS prevented MPB labeling of SecA and other proteins in all cases (supplemental Fig. S2). Second, to better understand the accessibility properties of the unlabeled group of mutants, we compared their labeling pattern in the absence and presence of 0.1% Triton X-100. This experiment indicated that these mutants could be divided into two subgroups. Cys-47, Cys-142, Cys-190, Cys-213, Cys-287, Cys-295, Cys-321, Cys-371, Cys-376, Cys-402, Cys-409, Cys-498, Cys-581, Cys-630, Cys-696, Cys-773, Cys-774, Cys-809, and Cys-827 all showed moderate to strong MBP labeling in the presence of Triton X-100 (supplemental Fig. S3). Because this experiment was performed on total cell protein rather than P300 fractions, it did not distinguish whether soluble or membrane-bound SecA (or both) was labeled in this case. In contrast, Cys-8, Cys-75, Cys-279, Cys-307, Cys-506, Cys-542, Cys-673, Cys-712, Cys-718, and Cys-744 all showed weak or no MPB labeling in the presence of Triton X-100. Thus approximately one-third of the unlabeled mutant group was inaccessible to MPB labeling *in vivo* under all conditions tested, presumably because of the bur-

TABLE 1
In vivo MPB labeling of monocysteine secA mutants

SecA Cys Residue[a]	Div Residue[b]	MPB Labeling[c]
C0	NA	U
8	7	U
47	45	U
59	57	M/S
75	73	U
104	102	M/S
142	140	U
190	188	U
213	211	U
225	223	W
226	224	M/S
233	231	M/S
256	243	M/S
265	252	M/S
279	266	U
287	274	U
292	279	W
295	282	U
300	NA	M/S
307	287	U
321	301	U
334	314	M/S
340	320	M/S
344	324	M/S
350	330	M/S
363	343	W
371	351	U
376	356	U
402	382	U
409	389	U
423	403	M/S
427	407	M/S
447	427	M/S
458[d]	438	M/S
470	450	W
498	478	U
506	486	U
514	494	M/S
518	498	M/S
530	NA	M/S
542	NA	U
581	532	U
597	548	M/S
600	551	M/S
630	581	U
640	591	M/S
641	592	M/S
656	607	M/S
661	612	W
673	624	U
696	647	U
712	663	U
718	671	U
734[d]	687	W
744	NA	U
753	702	M/S
773	722	U
774	723	U
787	736	W
809	758	U
827	776	U
833	782	M/S
858	798	M/S
896	836	M/S

NBF-I
NBF-II
PPXD
HWD
HSD
CTR

[a] The indicated monocysteine *secA* mutant was grown, MBP-labeled, and analyzed as described under "Experimental Procedures."
[b] Div residue indicates the *E. coli* SecA homologous residue of *B. subtilis* SecA. NA indicates not applicable, as certain "insertion" regions of *E. coli* SecA are not present in *B. subtilis* SecA. Residues lying within each *B. subtilis* SecA structural domain were color-coded according to the convention of Hunt *et al.* (8).
[c] The MPB labeling strength was quantified according to the following nomenclature: M/S, medium to strong labeling; W, weak labeling; U, unlabeled.
[d] BL21.19 (pT7secA-Cys-458) and BL21.19 (pT7secA-Cys-734) had lower plating efficiencies of 12 and 20%, respectively.

ying of the relevant cysteine residue within protein (*e.g.* SecA or SecYEG) or phospholipid. We note in this regard that a recent study indicated that multiple regions of SecA became buried after SecYEG and ATP binding, as assessed by acrylamide quenching of single tryptophan SecA mutants (43).

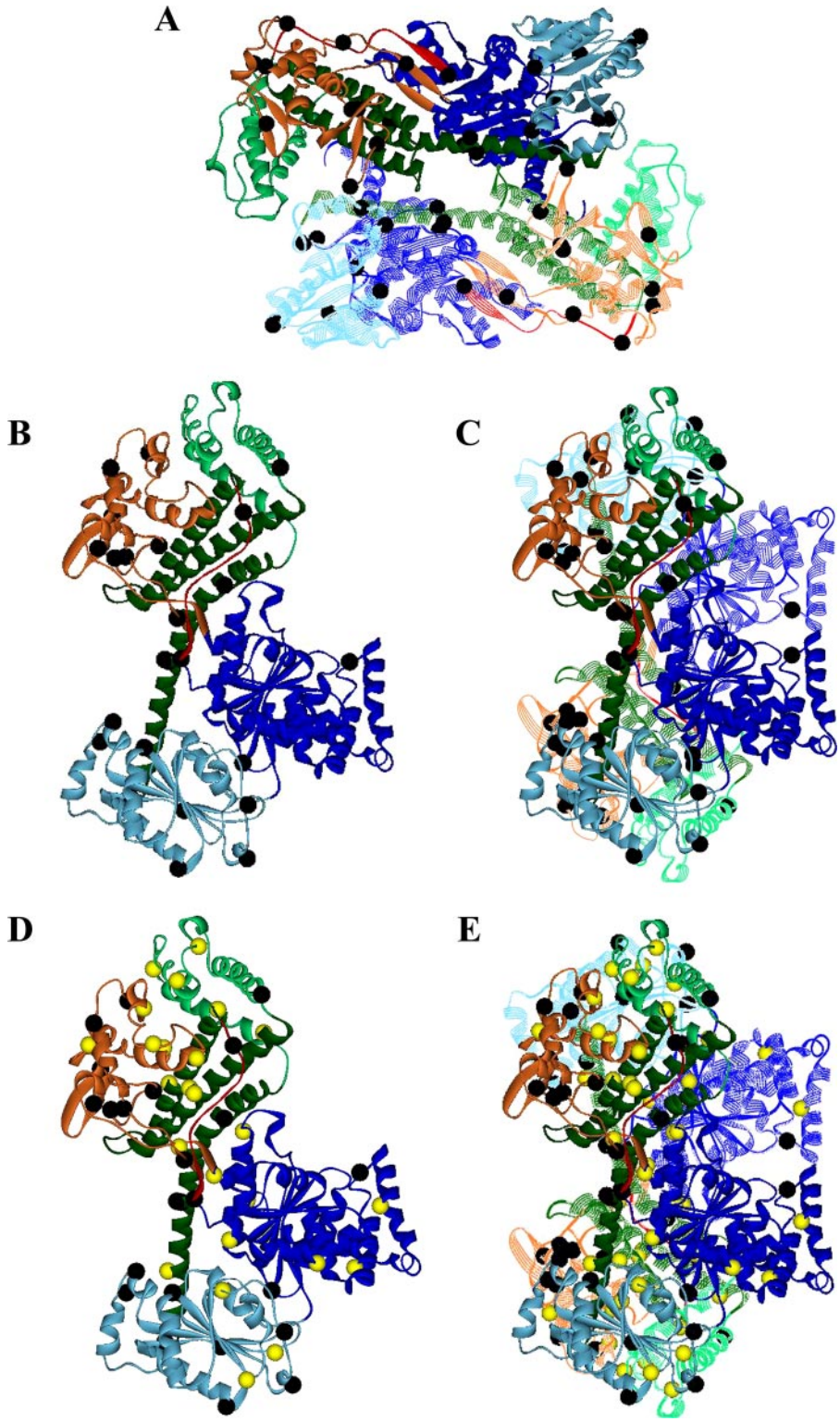

FIGURE 2. **Location of MPB-labeled residues on the *B. subtilis* SecA structure.** *A*, top view of the *B. subtilis* SecA dimer structure (8) utilizing the following domain-specific color code: *dark blue*, NBF-I; *light blue*, NBF-II; *orange*, PPXD; *dark green*, HSD; *light green*, HWD; *red*, CTR. M/S-labeled residues are shown as *black spheres*. *B* and *C*, side view of the *B. subtilis* SecA monomer and dimer, respectively. *D* and *E*, Similar to *B* and *C* except that both M/S- and unlabeled residues are depicted as *black* and *yellow spheres*, respectively.

been reported previously that membrane-bound SecA functions as a dimer (34, 45–47), although this result has been disputed in favor of a monomer action model and remains controversial (48, 49). The MBP labeling pattern was highlighted on both SecA protomers, because we were unable to distinguish whether any subunit labeling asymmetry was obtained in our study. We note that M/S-labeled residues are distributed throughout all structural domains of SecA with the possible exception of HWD, which contains only one such residue at the junction of the HWD and HSD domains. Most importantly, nearly all M/S-labeled residues lay on a single face of the dimer (shown in Fig. 2*A*; see below for a discussion of the exceptions and their significance). This result was most easily seen when the SecA protomers were viewed from the side, where the M/S-labeled residues clustered to one side of SecA (the *left side* of Fig. 2, *B* and *C*). PPXD, NBF-II, and CTR, which "sit" on top of the HSD scaffold, dominated the labeled side of SecA. Such an asymmetric labeling pattern argues strongly for the validity of our methodology and data set. By contrast, the unlabeled residues were distributed throughout the SecA structure (Fig. 2, *D* and *E*). This latter result was fully anticipated, because beyond the cytoplasmically oriented residues of SecA, other regions should be buried by their interaction with SecYEG or the membrane. In addition, localized protein fine structure may sterically block or retard MPB labeling chemistry.

In the front-to-front arrangement of the SecYEG dimer that was observed in the recent structure of the *E. coli* protein-conducting channel bound to a translating ribosome-nascent chain complex (29), the SecYEG dimer was cylindrical with a ~95-Å diameter and ~45-Å height, and it contained both translocationally active and inactive protomers. This observed size approximates the dimensions of the MPB-labeled face of the SecA dimer (~100 Å long and ~80 Å wide as viewed in Fig. 2*A*), suggesting that SecA may essentially "cover" the cytosolic face

Our results were represented on the highly homologous *B. subtilis* SecA dimer structure (8), although we caution the reader that it is uncertain how SecA structure changes upon SecYEG binding and membrane insertion (23, 43, 44). It has

of SecYEG in its bound and inserted state. In addition, the depth of MPB labeling of SecA (~15–20 Å) is suggestive of a more shallow insertion mechanism if no major SecA rearrangements were to occur during this process. Conclusive evidence on this latter point must clearly await better structural analysis of the SecA-SecYEG complex in its various translocation states. It is conceivable that some of our MPB-labeled residues were the result of periplasmic exposure of phospholipid-bound SecA protein, although this possibility seems unlikely because lipidic SecA has been described as peripheral in nature based on its dissociation from the membrane during sucrose gradient purification or by treatment with chaotropic reagents such as urea (15). Furthermore, SecYEG-bound SecA was found to be shielded from phopholipid acyl chains in a photo-cross-linking study (50), indicating that SecYEG-bound SecA does not appear to possess any sizable phospholipid-associated domain.

The PPXD and NBF-II domains showed considerable labeling bias (9 of 18 and 9 of 14 residues tested, respectively, were in the M/S group; Table 1), even given some variation in our coverage of SecA with monocysteine substitutions. This result is consistent with the proposed role of PPXD as the preprotein-binding domain of SecA that transfers bound preprotein to SecYEG (51–53). Both the 219–244 and 292–319 regions of SecA, which have been proposed to be critical for signal peptide binding (54, 55), contain M/S-labeled residues. NBF-II serves a regulatory role in SecA by controlling the ATPase cycle of NBF-I, which in turn controls SecA membrane cycling (22, 56–58). Thus SecYEG association by NBF-II and its proximity to the protein-conducting channel are likely to be important for coordination of this regulatory activity and SecA-SecYEG cross-talk. The three residues tested in the CTR domain (Cys-833, Cys-858, and Cys-896) were also found to label, consistent with previous results on the periplasmic accessibility of this region (20). CTR has been shown previously to be important for both SecB and phospholipid binding activities of SecA (12, 17). Thus this region of SecA may play both an early (SecB binding) as well as late step (regulating or optimizing a membrane-localized step) in protein translocation. Finally, significant labeling of the ~70-Å-long helix in HSD was observed as well. These regions may play more of a structural role in the correct positioning of SecA on SecYEG protein, given the importance of HSD as an organizing center for the other domains of SecA and associated activities.

Although most regions of NBF-I were distal to the labeled face of SecA and were not labeled, there were two exceptions to this rule: both Cys-59 and Cys-104 showed good labeling. Cys-59 is located within an amino-terminal extension "arm" of NBF-I, which would have to undergo significant conformational movement to bring it in proximity to the presumed SecA-SecYEG binding interface. Conformational movement of this region is supported by the occurrence of the *secA51*(*Ts*) mutation at residue 43, which results in a thermo-induced membrane "stuck" (inserted) phenotype for SecA protein (13, 22, 35, 58, 59). Cys-104 is within the Walker A motif of NBF-I that is essential for high affinity ATP binding along with regulating the preprotein binding and release and membrane insertion and retraction cycles of SecA (37, 60). One possible explanation for this observed result could be that this SecA region alternates between nucleotide-bound channel-distal and nucleotide-free channel-proximal states. For example, it has been suggested that ATP binding at NBF-I may drive the SecA membrane retraction step (8). Thus, in both cases, our study suggests conformational movements within NBF-I that need to be visually "captured" through appropriate structural techniques.

Our data provide support for an intriguing model to explain the mode of action of the two-pore translocon observed recently (29). In this model PPXD and NBF-II would serve to gate the active and inactive channels of the SecYEG dimer, respectively. This suggestion is consistent with the observed extensive MPB labeling pattern of these two comparably sized domains of SecA and also with their observed functions as preprotein binding and SecA-SecYEG regulatory domains, respectively (51, 52, 55–57). In this context PPXD and NBF-II labeling could occur on the same protomer or be divided between different protomers, depending on the SecA oligomeric state (monomer or dimer) as well as the SecYEG dimer orientation (front-to-front or back-to-back (29)).

In summary, our data demarcate a unique and extensive face of SecA primarily comprising PPXD, NBF-II, and CTR, which associates with SecYEG and is in fluid contact with the *trans* side of the membrane. The size of this region, although considerable, is not out of line with our current structural understanding of SecYEG protein architecture. For example, given the dimensions of the "closed state" of the proposed protein-conducting channel of the *M. jannaschii* SecY complex, a substantial portion of SecA would be needed to "plug" the large, funnel-like cavity, 20–25 Å in diameter, that lies at the channel entrance (25). Other regions of SecA not within this cavity could still be within fluid contact of the cavity. Furthermore, channel opening could accommodate additional regions of SecA as well as create further sites within fluid contact of the open channel. Our domain-specific and overall results provide ample opportunities to study this complex problem by further utilizing a combination of genetic, biochemical, and structural approaches.

Acknowledgments—We thank John Hunt for help in selecting the sites for cysteine-scanning mutagenesis, Susan Bankowski and Dominik Stoegermayer for construction of the monocysteine secA mutant collection and trial experiments utilizing RSO, and Amy Moffo for excellent technical assistance throughout this study.

REFERENCES

1. Veenendaal, A., van der Does, C., and Driessen, A. J. M. (2004) *Biochim. Biophys. Acta* **1694,** 81–95
2. Vrontou, E., and Economou, A. (2004) *Biochim. Biophys. Acta* **1694,** 67–80
3. Randall, L. L., and Hardy, S. J. (2002) *Cell. Mol. Life Sci.* **59,** 1617–1623
4. Pogliano, J. A., and Beckwith, J. (1994) *EMBO J.* **13,** 554–561
5. Duong, F., and Wickner, W. (1997) *EMBO J.* **16,** 4871–4879
6. Eichler, J., and Wickner, W. (1997) *Proc. Natl. Acad. Sci. U. S. A.* **94,** 5574–5581
7. Karamanou, S., Vrontou, E., Slanidis, G., Baud, C., Roos, T., Kuhn, A., Politou, A. S., and Economou, A. (1999) *Mol. Microbiol.* **35,** 1133–1145
8. Hunt, J. F., Weinkauf, S., Henry, L., Fak, J. J., McNicholas, P., Oliver, D. B., and Deisenhofer, J. (2002) *Science* **297,** 2018–2026
9. Sharma, V., Arockiasamy, A., Ronning, D. R., Savva, C. G., Holzenburg, A.,

Braunstein, M., Jacobs, W. R., and Sacchettini, J. C. (2003) *Proc. Natl. Acad. Sci. U. S. A.* **100,** 2243–2248
10. van Voorst, F., Vereyken, I. J., and de Kruijff, B. (2000) *FEBS Lett.* **486,** 57–62
11. Fekkes, P., van der Does, C., and Driessen, A. J. (1997) *EMBO J.* **16,** 6105–6113
12. Breukink, E., Nouwen, N., van Raalte, A., Mizushima, S., Tommassen, J., and de Kruijff, B. (1995) *J. Biol. Chem.* **270,** 7902–7907
13. Cabelli, R. J., Dolan, K. M., Qian, L., and Oliver, D. B. (1991) *J. Biol. Chem.* **266,** 24420–24427
14. Hartl, F.-U., Lecker, S., Schiebel, E., Hendrick, J. P., and Wickner, W. (1990) *Cell* **63,** 269–279
15. Eichler, J., Rinard, K., and Wickner, W. (1998) *J. Biol. Chem.* **273,** 21675–21681
16. Karamyshev, A., and Johnson, A. (2005) *J. Biol. Chem.* **280,** 37930–37940
17. Fekkes, P., de Wit, J. G., van der Wolk, J. P., Kimsey, H. H., Kumamoto, C. A., and Driessen, A. J. M. (1998) *Mol. Microbiol.* **29,** 1179–1190
18. Economou, A., and Wickner, W. (1994) *Cell* **78,** 835–843
19. Kim, Y. J., Rajapandi, T., and Oliver, D. (1994) *Cell* **78,** 845–853
20. Ramamurthy, V., and Oliver, D. (1997) *J. Biol. Chem.* **272,** 23239–23246
21. Eichler, J., and Wickner, W. (1998) *J. Bacteriol.* **180,** 5776–5779
22. Economou, A., Pogliano, J. A., Beckwith, J., Oliver, D. B., and Wickner, W. (1995) *Cell* **83,** 1171–1181
23. van der Does, C., Manting, E. H., Kaufmann, A., Lutz, M., and Driessen, A. J. M. (1998) *Biochemistry* **37,** 201–210
24. Scheuring, J., Braun, N., Nothdurft, L., Stumpf, M., Veenendaal, A., Kol, S., van der Does, C., Driessen, A. J. M., and Weinkauf, S. (2005) *J. Mol. Biol.* **354,** 258–271
25. van den Berg, B., Clemons, W. M., Collinson, I., Modls, Y., Hartmann, E., Harrison, S. C., and Rapoport, T. A. (2003) *Nature* **427,** 36–44
26. Meyer, T., Menetret, J.-F., Breitling, R., Miller, K., Akey, C., and Rapoport, T. (1999) *J. Mol. Biol.* **285,** 1789–1800
27. Breyton, C., Haase, W., Rapoport, T. A., Kuhbrandt, W., and Collinson, I. (2002) *Nature* **418,** 662–664
28. Manting, E. H., van der Does, C., Remigy, H., Engel, A., and Driessen, A. J. M. (2000) *EMBO J.* **19,** 852–861
29. Mitra, K., Schaffitzen, C., Shaikh, T., Tama, F., Simon, J., Brooks, C., Ban, N., and Frank, J. (2005) *Nature* **438,** 318–324
30. Cannon, K., Or, E., Clemons, W. M., Shibata, Y., and Rapoport, T. A. (2005) *J. Cell Biol.* **169,** 219–225
31. Pohlschroder, M., Prinz, W. A., Hartmann, E., and Beckwith, J. (1997) *Cell* **91,** 563–566
32. van Geest, M., and Lolkema, J. (2000) *Microbiol. Mol. Biol. Rev.* **64,** 13–33
33. Studier, W. F., Rosenberg, A. H., Dunn, J. J., and Dubendorff, J. W. (1990) *Methods Enzymol.* **185,** 60–89
34. Jilaveanu, L. B., Zito, C. R., and Oliver, D. (2005) *Proc. Natl. Acad. Sci. U. S. A.* **102,** 7511–7516
35. Schmidt, M. G., Rollo, E. E., Grodberg, J., and Oliver, D. B. (1988) *J. Bacteriol.* **170,** 3404–3414
36. Sadaie, Y., Takamatsu, H., Nakamura, K., and Yamane, K. (1991) *Gene* **98,** 101–105
37. Mitchell, C., and Oliver, D. B. (1993) *Mol. Microbiol.* **10,** 483–497
38. Bayer, E., Zalis, M., and Wilchek, M. (1985) *Anal. Biochem.* **149,** 529–536
39. Loo, T., and Clarke, D. (1995) *J. Biol. Chem.* **270,** 843–848
40. Stewart, J., and Hermodson, M. (2003) *J. Bacteriol.* **185,** 5234–5239
41. van der Does, C., de Keyzer, J., van der Laan, M., and Driessen, A. (2003) *Methods Enzymol.* **372,** 86–98
42. Zito, C. R., and Oliver, D. (2003) *J. Biol. Chem.* **278,** 40640–40646
43. Natale, P., den Blaauwen, T., van der Does, C., and Driessen, A. J. M. (2005) *Biochemistry* **44,** 6424–6432
44. van der Does, C., den Blaauwen, T., de Wit, J. G., Manting, E., Groot, N., Fekkes, P., and Driessen, A. J. M. (1996) *Mol. Microbiol.* **22,** 619–629
45. Driessen, A. (1993) *Biochemistry* **32,** 13190–13197
46. de Keyzer, J., van der Sluis, E. O., Spelbrink, R. E. J., Nijstad, N., de Kruijff, B., Nouwen, N., van der Does, C., and Driessen, A. J. M. (2005) *J. Biol. Chem.* **280,** 35255–35260
47. Jilaveanu, L. B., and Oliver, D. (2006) *J. Bacteriol.* **188,** 335–338
48. Or, E., Navon, A., and Rapoport, T. (2002) *EMBO J.* **21,** 4470–4479
49. Or, E., Boyd, D., Gon, S., Beckwith, J., and Rapoport, T. A. (2004) *J. Biol. Chem.* **280,** 9097–9105
50. van Voorst, F., van der Does, C., Brunner, J., Driessen, A. J. M., and de Kruijff, B. (1998) *Biochemistry* **37,** 12261–12268
51. Kimura, E., Akita, M., Matsuyama, S.-I., and Mizushima, S. (1991) *J. Biol. Chem.* **266,** 6600–6606
52. Papanikou, E., Karamanou, S., Baud, C., Frank, M., Sianidis, G., Keramisanou, D., Kalodimos, C., Kuhn, A., and Economou, A. (2005) *J. Biol. Chem.* **280,** 43209–43217
53. Wang, L., Miller, A., Rusch, S., and Kendall, D. (2004) *Biochemistry* **43,** 13185–13192
54. Baud, C., Karamanou, S., Sianidis, G., Vrontou, E., Politou, A. S., and Economou, A. (2002) *J. Biol. Chem.* **277,** 13724–13731
55. Musial-Siwek, M., Rusch, S., and Kendall, D. (2005) *Biochemistry* **44,** 13987–13996
56. Nakatogawa, H., Mori, H., and Ito, K. (2000) *J. Biol. Chem.* **275,** 33209–33212
57. Sianidis, G., Karamanou, S., Vrontou, E., Boulias, K., Repanas, K., Kyrpides, N., Politou, A. S., and Economou, A. (2001) *EMBO J.* **20,** 961–970
58. Rajapandi, T., and Oliver, D. (1996) *Mol. Microbiol.* **20,** 43–51
59. Oliver, D., and Beckwith, J. (1981) *Cell* **25,** 765–772
60. Matsuyama, S., Kimura, E., and Mizushima, S. (1990) *J. Biol. Chem.* **265,** 8760–8765